ACCRETION ASSISTED INSPIRALS

NEAR GALACTIC NUCLEI

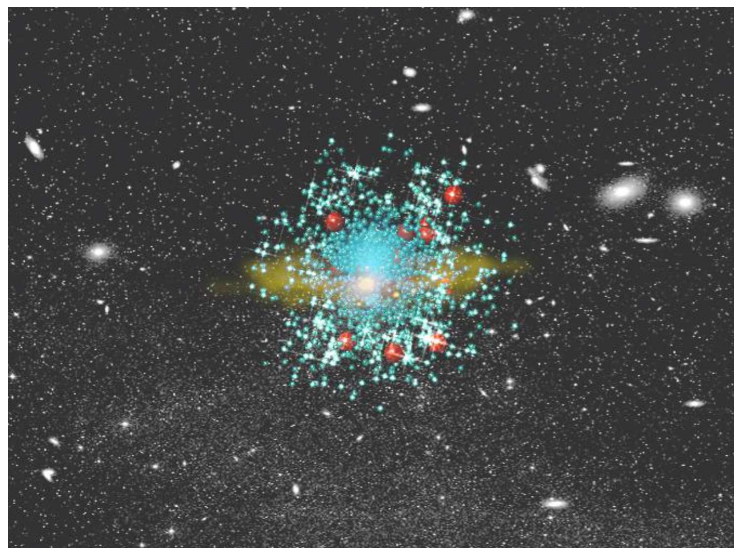

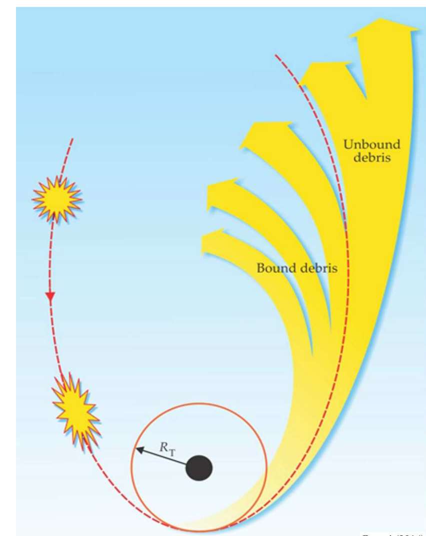

Vladimír Karas

Astronomical Institute of the Czech Academy of Sciences, Prague

Star-disc interaction

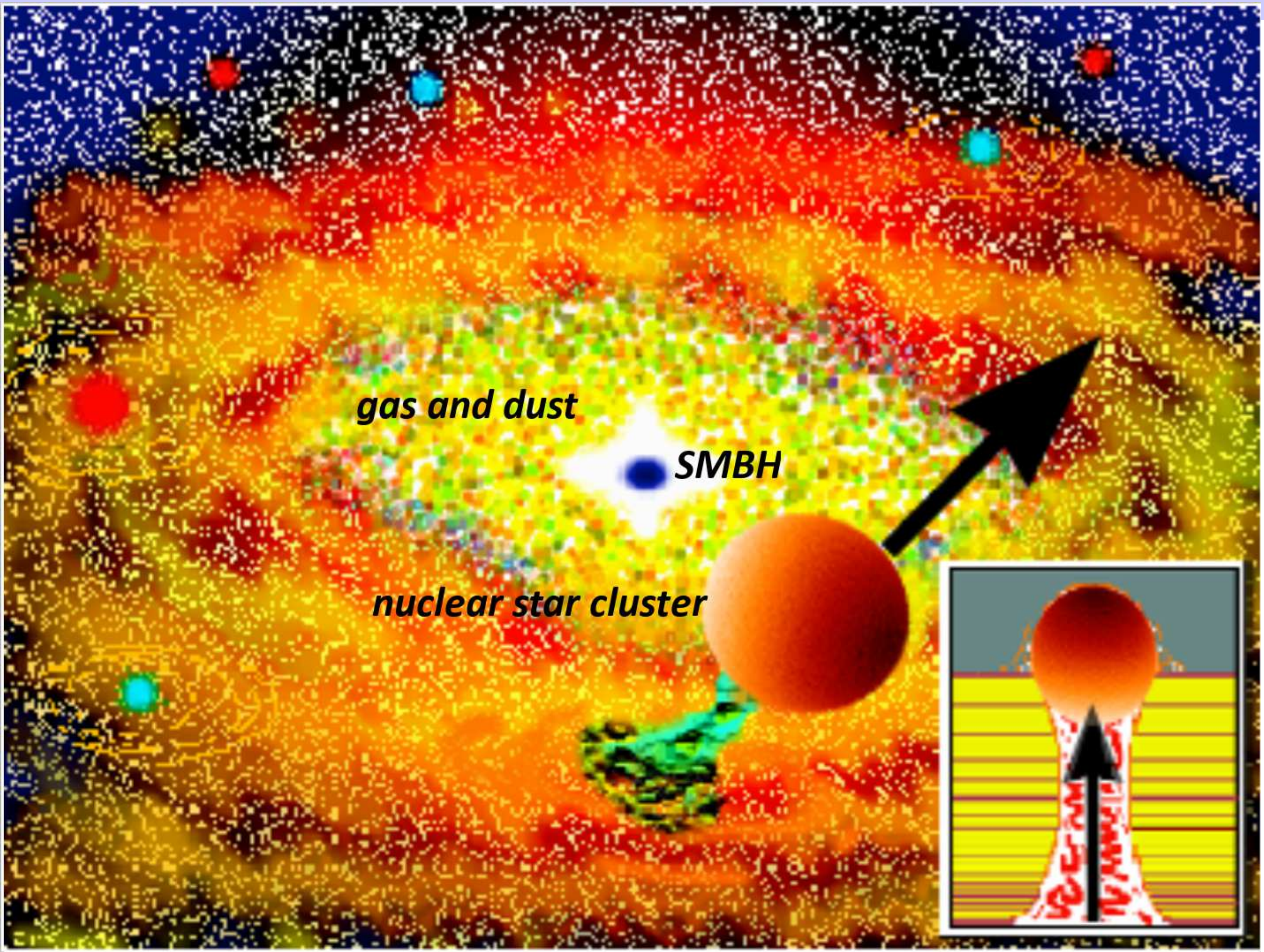

Model

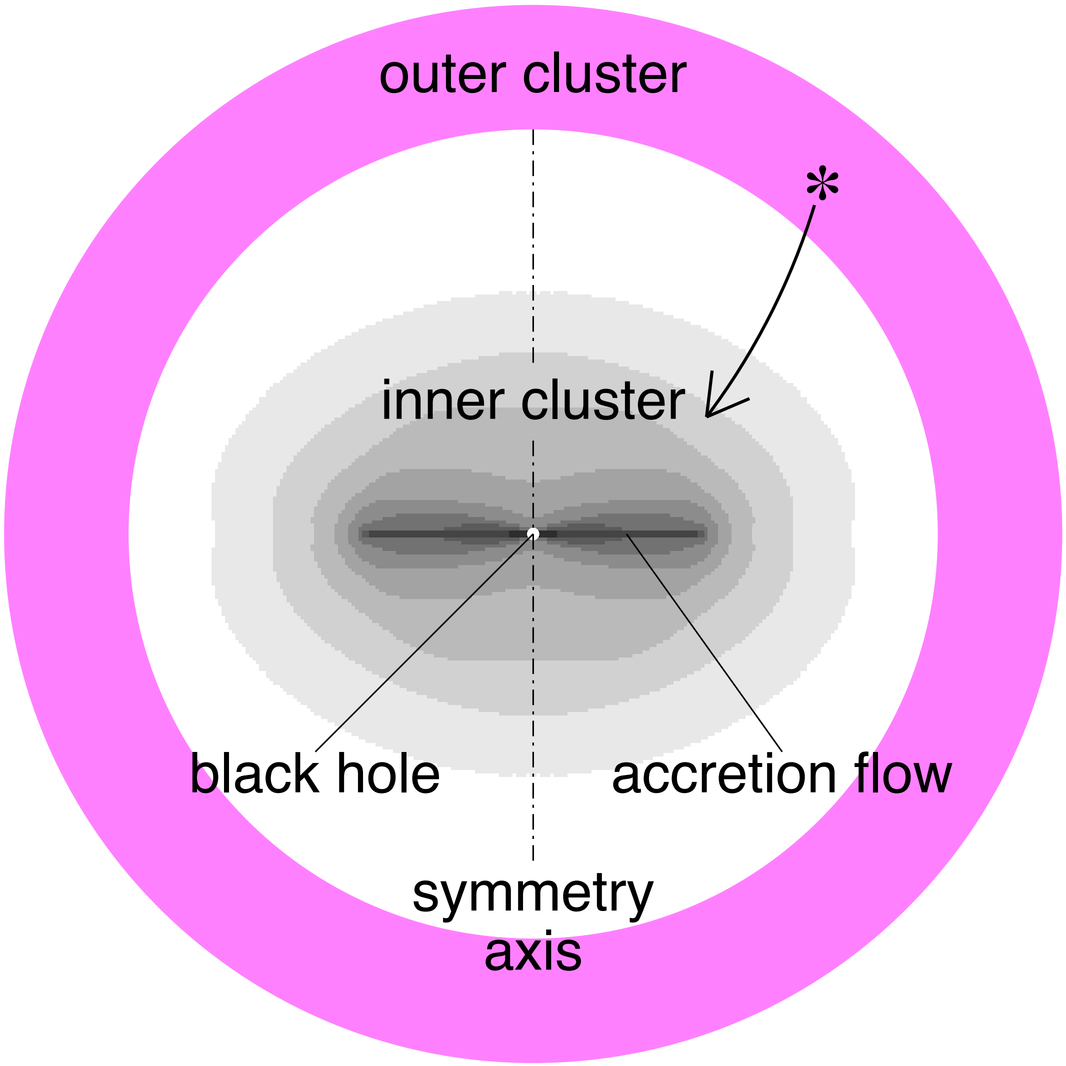

- Black hole
  $M_{\mathrm{BH}} \approx 10^3 - 10^8 M_\odot$

- Accretion flow
  $\Sigma_{\mathrm{d}} \propto r^s$
  $R_{\mathrm{d}} \approx 10^4 R_{\mathrm{g}} \approx 0.1\,\mathrm{pc}$

- 'Outer' cluster
  $n(r) = n_0 (r/r_{\mathrm{h}})^{-7/4}$
  $r_{\mathrm{h}} \approx 10\,\mathrm{pc}$
  $n_0 \approx 10^6 - 10^8 \mathrm{pc}^{-3}$

- 'Inner' cluster…

Kozai–Lidov mechanism

- evolution of a hiearchical triple system $m_0 > m_1 > m_2$

  Lidov 1961: Earth > Moon > satellite

  Kozai 1962: Sun > Jupiter > asteroid

- secular evolution of the orbital elements e, i and ω
- ‘averaging’ technique of the Hamiltonian perturbation theory allows to get rid of ‘fast’ variable (mean anomaly)
- integrals of motion: a, $C_1 \equiv \sqrt{1-e^2}\cos i$ and $\bar{V}_{\rm d}$
- motion of a star in the gravitational field of the central mass and an axisymmetric perturbation (ring, torus, disc. . .)

Kozai equations

Newtonian framework

$$T_{\rm K}\sqrt{1-e^2}\,\frac{\mathrm{d}i}{\mathrm{d}t} = -5e^2\sin i\,\cos i\,\sin\omega\,\cos\omega$$

$$T_{\rm K}\sqrt{1-e^2}\,\frac{\mathrm{d}e}{\mathrm{d}t} = 5e(1-e^2)\sin^2 i\,\sin\omega\,\cos\omega$$

$$T_{\rm K}\sqrt{1-e^2}\,\frac{\mathrm{d}\omega}{\mathrm{d}t} = 2(1-e^2)+5(e^2-\sin^2 i)\sin^2\omega$$

$$T_{\rm K} \equiv \frac{4}{3}\frac{M_{\rm BH}}{M_{\rm d}}\left(\frac{R_{\rm d}}{a}\right)^3 P$$

$\bar{V}_{\rm d}$ = const., *perturbation potential for a disc*

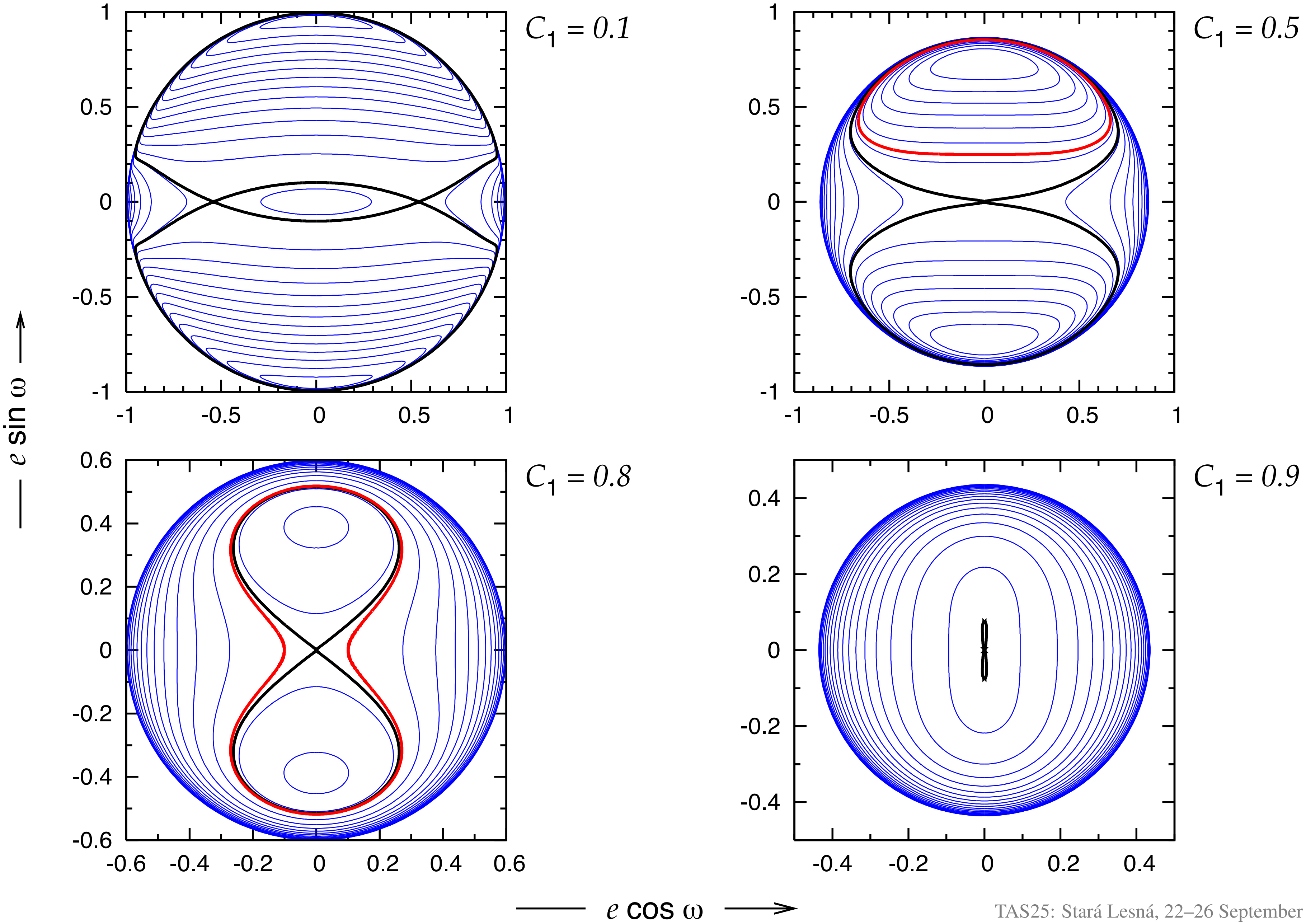

Damping effect of the relativistic pericentre advance

- Characteristic timescales:

$$T_{\mathrm{K}} = \frac{4}{3}\frac{M_{\mathrm{BH}}}{M_{\mathrm{d}}}\left(\frac{R_{\mathrm{d}}}{a}\right)^{3} P \qquad \text{vs.} \qquad T_{\mathrm{E}} = \frac{1}{3}\frac{a(1-e^{2})}{R_{\mathrm{g}}} P$$

- Kozai oscillations are suppressed for

$$a < a_{\mathrm{min}} \approx \left(\frac{M_{\mathrm{BH}}}{M_{\mathrm{d}}}\right)^{2} \left(\frac{R_{\mathrm{d}}}{R_{\mathrm{g}}}\right)^{6/7} \left(\frac{R_{\mathrm{min}}}{R_{\mathrm{g}}}\right)^{-1/7} R_{\mathrm{g}}$$

... prominent effect in case of extreme relativistic TDE *(Karas & Šubr, 2007, A&A)*

Effect of an extended star cluster

Stellar cusp in the sphere of influence of the central black hole

- Bahcall & Wolf (1976): $\rho(r) \propto r^{-7/4}$
- Galactic centre:

$$\rho(r) \approx 1.2 \times 10^6 \left(\frac{r}{0.4\mathrm{pc}}\right)^{-\alpha} M_\odot \, \mathrm{pc}^{-3}$$

$$\alpha = \begin{cases} 1.4 & r \lesssim 0.4\mathrm{pc} \\ 2.0 & r \gtrsim 0.4\mathrm{pc} \end{cases}$$

$$V_c(r) \propto \begin{cases} r^{2-\alpha} & \alpha < 2 \\ \ln(r) & \alpha = 2 \end{cases}$$

In the Galactic centre

molecular torus (ring):

$$
\begin{aligned}
M_{\mathrm{d}} &= 0.1 M_{\mathrm{BH}} \\
R_{\mathrm{d}} &= 1.6\,\mathrm{pc}
\end{aligned}
$$

star cluster:

$$
\begin{aligned}
\rho(r) &\propto r^{-1.75} \\
M_{\mathrm{c}}(1.6\mathrm{pc}) &= M_{\mathrm{BH}}
\end{aligned}
$$

$$
\begin{aligned}
\mathcal{F}(R_{\mathrm{t}}) &\approx 3 \times 10^{-4} \\
N &\approx 100
\end{aligned}
$$

(clockwise) stellar disc:

$$
\begin{aligned}
M_{\mathrm{d}} &= 0.01 M_{\mathrm{BH}} \\
R_{\mathrm{in}} &= 0.03\,\mathrm{pc} \\
R_{\mathrm{out}} &= 0.3\,\mathrm{pc} \\
\Sigma(r) &\propto r^{-2}
\end{aligned}
$$

star cluster:

$$
\begin{aligned}
\rho(r) &\propto r^{-1.4} \\
M_{\mathrm{c}}(0.4\mathrm{pc}) &= 0.2 M_{\mathrm{BH}}
\end{aligned}
$$

$$
\begin{aligned}
\mathcal{F}(R_{\mathrm{t}}) &\approx 2 \times 10^{-3} \\
N &\approx 100
\end{aligned}
$$

Exemplary model

- mass-sigma relation: $\sigma \approx 20\,(M_{\mathrm{BH}}/10^4 M_\odot)^{1/4}\,\mathrm{km\,s^{-1}}$
- characteristic radius of the star cluster: $R_{\mathrm{h}} = GM_{\mathrm{BH}}/\sigma^2$
- $R_{\mathrm{d}} = R_{\mathrm{h}}\,,\ 0.04R_{\mathrm{h}} \le a \le 0.4R_{\mathrm{h}}$
- $M_{\mathrm{d}} = 0.01M_{\mathrm{BH}}\,,\ M_{\mathrm{c}} = M_{\mathrm{BH}}\,,\ M_* = M_\odot\,,\ R_* = R_\odot$

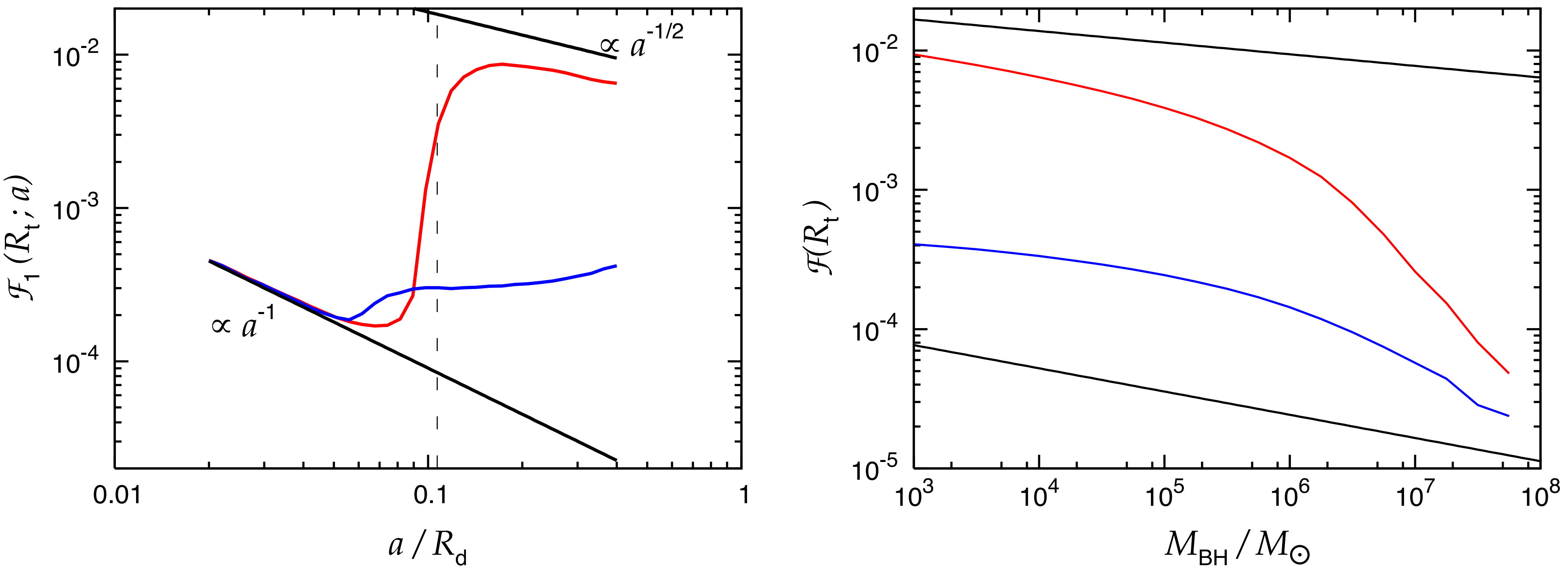

EMRI vs. TDE

Millihertz oscillations near the innermost orbit of a supermassive black hole

Megan Masterson, Erin Kara, Christos Panagiotou, William N. Alston, Joheen Chakraborty, Kevin Burdge, Claudio Ricci, Sibasish Laha, Iair Arcavi, Riccardo Arcodia, S. Bradley Cenko, Andrew C. Fabian, Javier A. García, Margherita Giustini, Adam Ingram, Peter Kosec, Michael Loewenstein, Eileen T. Meyer, Giovanni Miniutti, Ciro Pinto, Ronald A. Remillard, Dev R. Sadaula, Onic I. Shuvo, Benny Trakhtenbrot & Jingyi Wang

Nature **638**, 370–375 (2025) | Cite this article

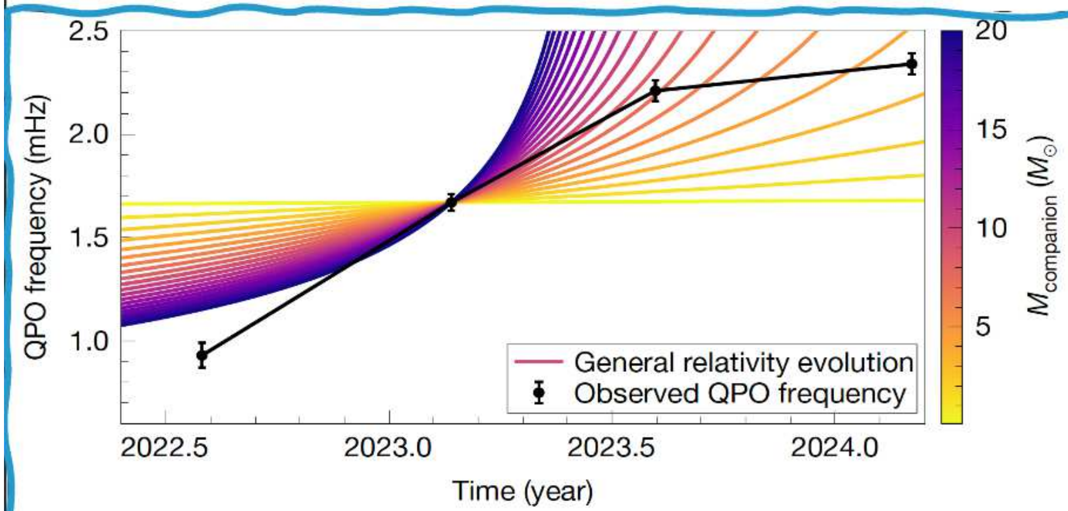

Fig. 3 | Evolution of the QPO frequency over time. The black points show the observed QPO frequency and 1σ error bars, obtained by fitting an additional Lorentzian for the QPO. The coloured lines show the expected evolution of an extreme-mass-ratio companion under general relativity alone, assuming a circular orbit (eccentricity of $e = 0$) and companion masses ranging from $0.1\,M_\odot$ to $20\,M_\odot$. The colour bar shows the mass distribution. The general relativity model was chosen to match the QPO frequency in February 2023, as these were the data with the most significant detection and the lowest uncertainty on the QPO frequency. General relativity alone for an orbiting companion cannot account for the frequency evolution seen in 1ES 1927+654.

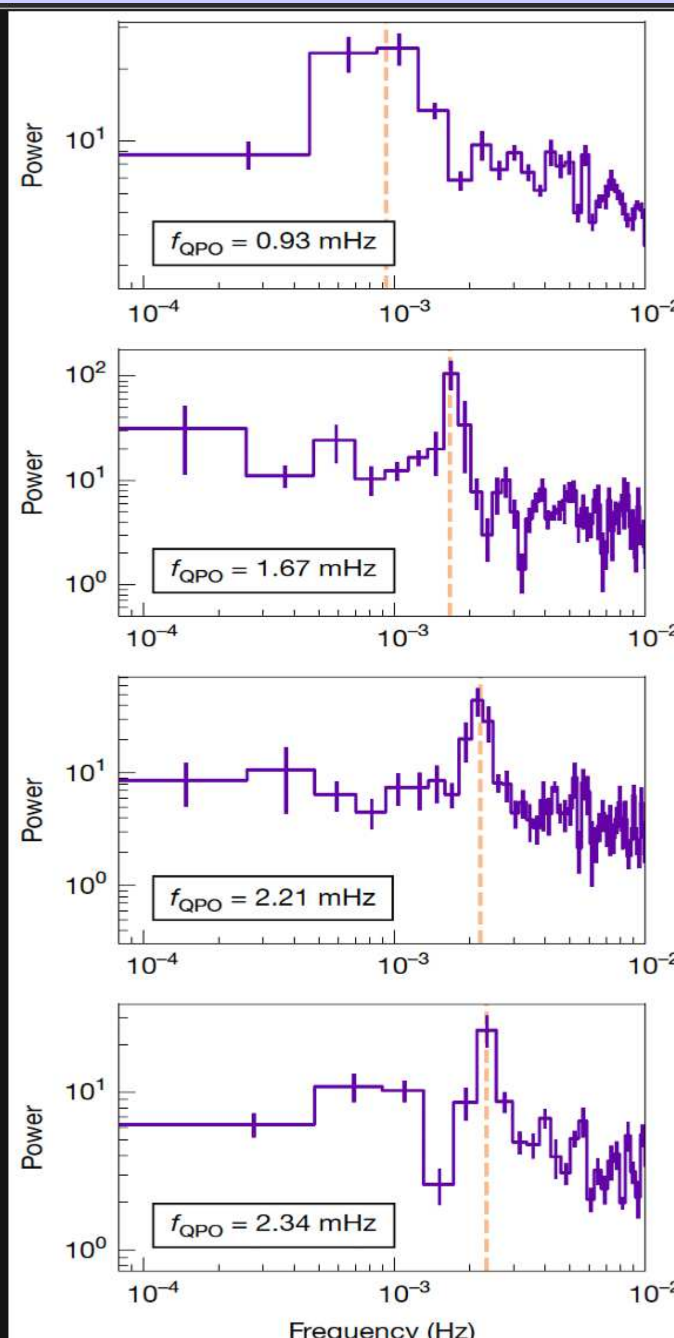

Thank you!

References

- Gravitating discs around black holes
  (Karas, Huré, Semerák, 2004, CQG 21, 1;
  Karas & Šubr, 2010, IAU Symp. 267, 332)

- Star-disc interactions in a galactic centre and oblateness of the inner stellar cluster
  (Šubr, Karas, & Huré, 2004, MNRAS 345, 1177)

- Stellar Transits across a Magnetized Accretion Torus as a Mechanism for Plasmoid Ejection
  Suková, Zajaček, Witzany, & Karas, 2021, ApJ 917, id. 43

Discussion slides – Two-body Hamiltonian

Carthesian coordinates:

$$\mathcal{H} = \frac{1}{2}\left(v_1^2 + v_2^2 + v_3^2\right) - \frac{\mathcal{G}\,(m_0 + m_1)}{\sqrt{x_1^2 + x_2^2 + x_3^2}}$$

Delaunay variables:

$$\mathcal{H} = -\frac{\mathcal{G}^2(m_0 + m_1)^2}{2L^2}$$

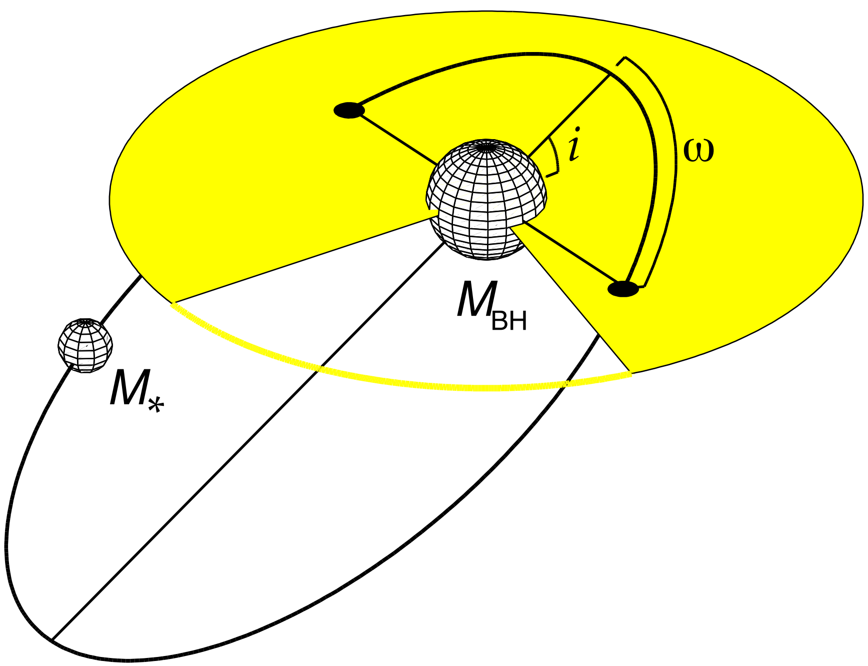

$$L = \sqrt{\mathcal{G}(m_0 + m_1)a} \qquad l = M$$

$$G = L\sqrt{1 - e^2} \qquad g = \omega$$

$$H = G\cos i \qquad h = \Omega$$

Tidal disruptions

- enhanced tidal disruptions due to the eccentricity oscillations
- supply of gas for accretion discs; food for black holes

$$R_{\rm t} = \left(\frac{M_{\rm BH}}{M_*}\right)^{1/3} R_* = 47 \left(\frac{M_{\rm BH}}{10^6 M_\odot}\right)^{-2/3} \left(\frac{M_*}{M_\odot}\right)^{-1/3} \left(\frac{R_*}{R_\odot}\right) R_{\rm g}$$

- characteristic radius of the stellar cluster $\sim 10^6 R_{\rm g} \Longrightarrow$ extreme eccentricities needed
- $\mathcal{F}(R_{\rm min})$: fraction of stars from an ensemble with given (initial) distribution of orbital elements $D_{\rm f}(a, e, i, \omega)$ that pass the centre within $R_{\rm min}$.

Discussion slides – Eccentric mergers

AGN as potential factories for eccentric black hole mergers

Nature | Vol 603 | 10 March 2022 | 237

https://doi.org/10.1038/s41586-021-04333-1
Received: 8 October 2020

J. Samsing[1]✉, I. Bartos[2], D. J. D'Orazio[1], Z. Haiman[3], B. Kocsis[4,5], N. W. C. Leigh[6,7], B. Liu[1], M. E. Pessah[1] & H. Tagawa[8]

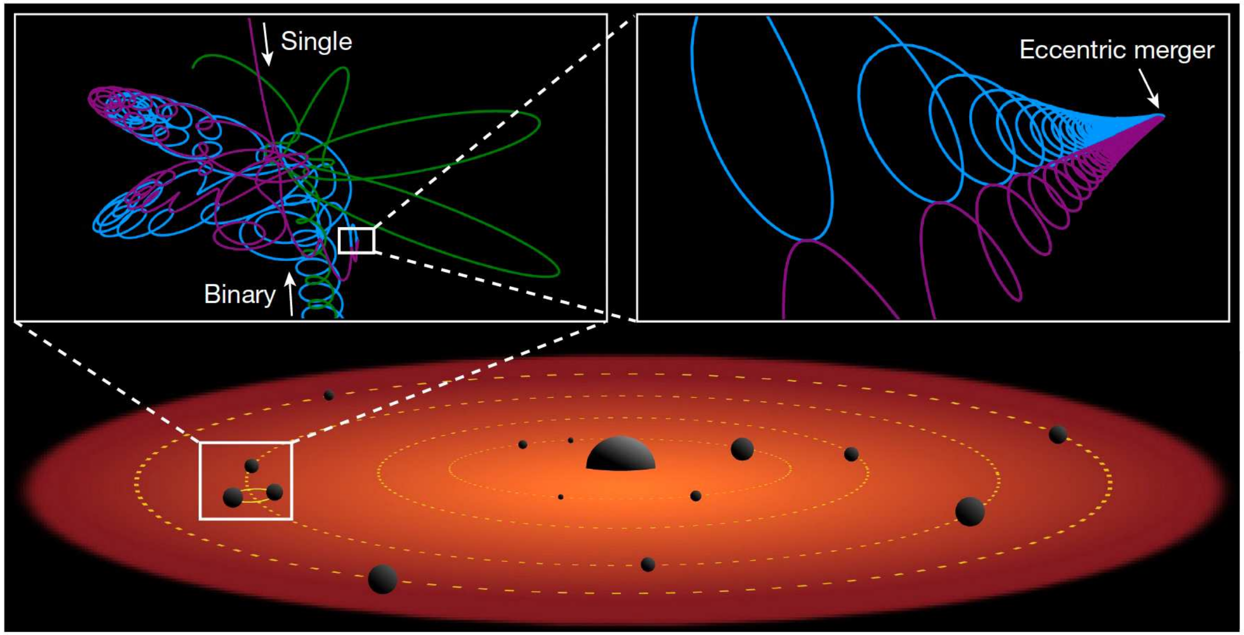

Fig. 1 | Illustration of an eccentric LIGO-Virgo source forming in an AGN disk. Bottom, AGN disk (not to scale) with its central supermassive black hole and a population of smaller orbiting black holes. These smaller black holes occasionally pair up to form binary black holes, which often undergo scatterings with the single-black-hole population. Top, outcome of a [50 $M_\odot$, 80 $M_\odot$] binary black hole interacting with an incoming [70 $M_\odot$] black hole, which results in a [80 $M_\odot$, 70 $M_\odot$] binary black hole merger during the interaction, with an eccentricity of about 0.5 in LIGO-Virgo.

Case of subgiant star stripped to its helium core

THE ASTROPHYSICAL JOURNAL LETTERS, 987:L11 (10pp), 2025 July 1 Olejak et al.

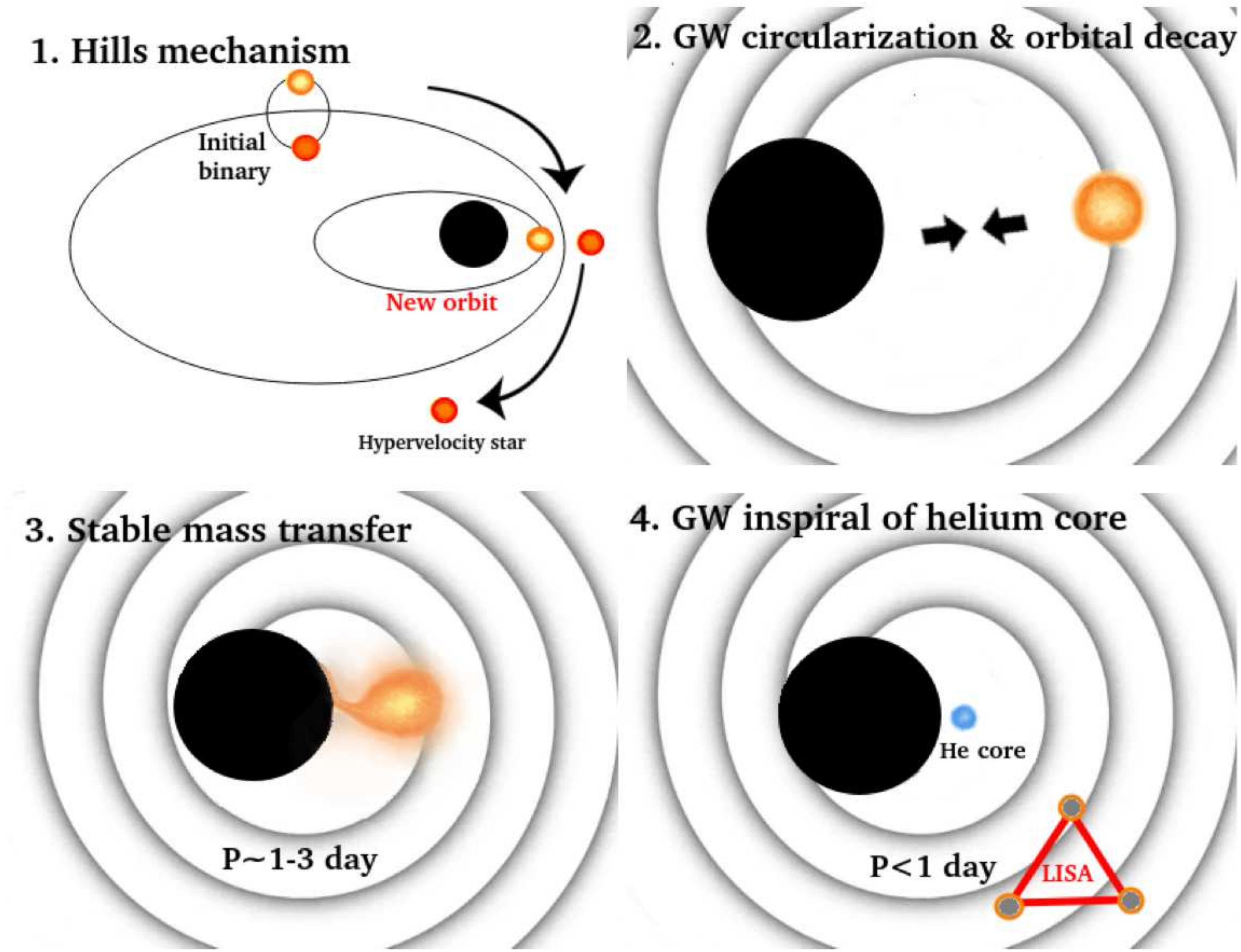

Figure 1. Cartoon representation of four relevant evolutionary stages of the system. Top left panel: the initial binary star system enters the Hill sphere of an SMBH and is disrupted. One star becomes gravitationally bound to the SMBH in an eccentric orbit, while the other is ejected from the Galactic nucleus, becoming a hypervelocity star. Top right panel: the orbit of the star bound to the SMBH gradually shrinks and circularizes owing to the strong emission of GWs. Bottom left panel: as the orbit continues to tighten, a subgiant star fills its Roche lobe, initiating a phase of long, stable mass transfer onto the SMBH. Bottom right panel: the star is eventually stripped of its hydrogen envelope during the mass transfer process. The system continues to shrink owing to GW emission, eventually entering the LISA frequency band as a detectable GW source.